[redacted]

[redacted]

RM E51K08

C-1

NACA

RESEARCH MEMORANDUM

EXPERIMENTAL INVESTIGATION OF THE HEAT-TRANSFER CHARACTERISTICS OF AN AIR-COOLED SINTERED POROUS TURBINE BLADE

By Louis J. Schafer, Jr., Edward R. Bartoo, and Hadley T. Richards

Lewis Flight Propulsion Laboratory
Cleveland, Ohio

NATIONAL ADVISORY COMMITTEE FOR AERONAUTICS

WASHINGTON
February 5, 1952

[redacted]

NATIONAL ADVISORY COMMITTEE FOR AERONAUTICS

RESEARCH MEMORANDUM

EXPERIMENTAL INVESTIGATION OF THE HEAT-TRANSFER CHARACTERISTICS OF AN AIR-COOLED SINTERED POROUS TURBINE BLADE

By Louis J. Schafer, Jr., Edward R. Bartoo, and Hadley T. Richards

SUMMARY

An experimental investigation was conducted on a static cascade to determine the heat-transfer characteristics of an air-cooled, sintered, porous, stainless-steel turbine blade in the gas temperature range from 300° to 1000° F. It was found that transpiration cooling was a very effective means of cooling the midchord regions of the turbine blade investigated but, because of the high flow resistance of the relatively long flow paths in the leading and trailing edges, these regions received only negligible amounts of coolant, and high local-wall temperatures resulted. As an example of the cooling effectiveness at the midchord region, the coolest temperature on the porous blade was compared with the coolest temperature on a convection-cooled blade for a gas temperature of approximately 1000° F, a coolant temperature of approximately 100° F and a ratio of coolant-to-gas flow of 0.04. The midchord temperature of the transpiration-cooled blade was about 170° F, whereas the midchord temperature of the convection-cooled blade was about 530° F. The expected high effectiveness of transpiration cooling is thus demonstrated and the possibility of a marked increase in turbine-inlet gas temperature or a reduction in the cooling-air flow requirements is realized.

A successful correlation of blade-wall temperature data obtained at different combustion-gas temperatures was made. As was expected from the ANALYSIS section, the correlation procedure did not eliminate the effects of combustion-gas Reynolds number.

Blade-wall temperatures were calculated using an approximate theory for turbulent-flow transpiration cooling and were compared with measured blade-wall temperatures. The calculated temperatures were generally higher than the measured temperatures.

INTRODUCTION

The application of transpiration cooling to turbine blades is being investigated at the NACA Lewis laboratory. This method of cooling has provided a very effective method of cooling objects such as rocket nozzles (reference 1) that are exposed to a hot gas stream. A study of the mechanism of transpiration cooling, a review of some earlier investigations, and a discussion of the problems of applying this method of cooling to turbine blades has been published (reference 2). Theories of the heat-transfer process in transpiration-cooled materials for laminar boundary-layer flow on the hot-gas side have also been developed and published for both constant- and variable-fluid properties in the boundary layer and for various types of pressure distribution in the flow along the porous walls (references 3 and 4). Only approximate solutions have been obtained for turbulent boundary-layer flow and these are dependent upon numerous simplifying assumptions. Solutions for this case are reported in references 5 and 6 and a comparison with experimental data on flow through porous wall tubes has been made.

In applying transpiration cooling to turbine blades, two major cooling problems exist. The first problem is that of supplying coolant to long thin leading- and trailing-edge sections the geometry of which will not tolerate coolant-supply passages. The second problem is that of obtaining adequate cooling of all parts of a blade with a pressure gradient existing around its perimeter. The purpose of the present report is to present the results of an investigation on a turbine blade manufactured by a powder metallurgy technique, to evaluate some of the design and fabrication problems that may occur with this type of blade cooling, and to determine to what extent established heat-transfer relations apply to the transpiration cooling of a typical turbine blade.

Data were obtained over ranges of gas Reynolds numbers from 107,000 to 293,000, gas temperatures from 300° to 1000° F, and local cooling-air to combustion-gas mass-velocity ratios from 0.001 to 0.036.

The blades used in this investigation were made at Stevens Institute of Technology under the sponsorship of the NACA for the development of the technique of fabricating porous sintered stainless-steel turbine blades.

APPARATUS

Porous Blades

The porous blades used in this investigation were nontwisted and nontapered with a 1.97-inch chord, a 3.5-inch span, and a 0.12-inch nominal wall thickness (fig. 1). The blades were made by a powdered-metal technique from AISI type 301 stainless-steel powder as explained in reference 7. The external profile was the same as that of the root section of the rotor blades of a current jet engine. Photographs showing several views of the blades are presented in figure 2.

In the die in which these blades were made, pressure was applied from both ends in the spanwise direction. Friction between the metal powder and the walls of the die was appreciable in the thin sections and resulted in wide variations in porosity in the blade. The porosity in percent is defined as $1 - \frac{\text{density of porous compact}}{\text{density of parent material}} \times 100$. The average porosity at the ends of the blade was approximately 12 percent and approximately 30 percent at the center of the span. These values were determined by cutting a blade into sections approximately 1/2 inch wide in the spanwise direction and comparing the weight of each section with the weight of an equal volume of solid parent metal.

Test Facility

In the test facility, combustion air passed successively through an orifice, a combustion chamber, a plenum chamber, the test section, and into the exhaust system. A standard jet-engine combustion chamber was used in order to obtain gas temperatures from 300° to 1000° F. The inlet duct to the test section was equipped with a bellmouth to insure a uniform velocity profile at the cascade entrance. The setup was insulated against heat loss through the duct walls from just downstream of the combustor to just downstream of the test section.

A cascade of seven blades was placed in the test section as shown in figure 3. A porous blade was installed as the center blade, which was the only blade cooled. The cooling air to the porous blade was supplied at room temperature through a pressure regulator, a filter, a rotameter, and finally through a manifold section into the blade.

The manifold section, which is shown in figure 4, was formed from 1/32-inch Inconel tubing. The opposite end of the blade was capped. The other six blades in the cascade were nonporous with the same profile.

Instrumentation

Blade. - The instrumentation of the porous blade for the heat-transfer investigation consisted of eight thermocouples in the blade wall around the perimeter at the locations shown in figure 1. The thermocouples were made of 30 gage (0.010 in. diam) calibrated chromel-alumel wire. The leads from the thermocouples were threaded through 0.040-inch diameter double-bore ceramic tubes which were inserted in holes in the blade wall drilled from the end of the blade. The thermocouples in the wall were installed as nearly as possible in the center of the wall and those in the leading and trailing edges were installed along the camber line.

The presence of the thermocouple tubes in the blade walls in the midchord and leading-edge regions probably has little effect on the coolant flow around the thermocouple junctions because the air flows around the tubes as in a low-velocity air stream. However, in the trailing edge, the flow that is blocked by the tubes amounts to 9, 12, and 25 percent, respectively, for thermocouples 4, 5, and 6.

Test facility. - The instrumentation in the test section is shown in figure 5. It consisted of a thermocouple and a static-pressure probe in the cooling-air passage of the porous blade at the midspan location. The low velocities encountered (160 ft/sec, maximum) rule out any appreciable wall effect on the static-pressure probe. Six equally spaced static taps were placed in the walls of the inlet-combustion-gas duct upstream of the cascade. Three thermocouples and three pressure probes located in the plenum chamber upstream of the test section indicated the total temperature and pressure of the gas stream.

TEST PROCEDURE

The effectiveness of the cooling of the porous blade was determined by measuring the blade-wall temperatures for a series of cooling-air weight flows at several constant combustion-gas weight flows and temperatures. The conditions covered in this investigation are given in the following table:

Combustion-gas temperature (°F)	Total gas weight flow (lb/sec)	Gas-inlet Mach number	Cooling-air temperature (°F)	Cooling-air weight flow per blade (lb/sec)
1000	4	0.45	100	0.011-0.043
600	4	.40	95	.011- .044
300	4	.37	80	.011- .044
300	3	.29	80	.013- .043
300	6	.46	80	.007- .045
300	7	.54	80	.011- .044

The range of hot-gas-inlet Reynolds numbers covered was from 107,000 to 293,000. These Reynolds numbers were based on the gas velocity at the cascade inlet; the gas properties were evaluated at the static temperature at the cascade inlet; and the characteristic dimension used was the blade perimeter divided by π.

The porous blade used in the heat-transfer investigation was the one which was calibrated at room temperature as described in reference 7.

ANALYSIS

Determination of Local Cooling-Air-Flow Distribution

A calibration to determine the local cooling-air flow variation around the blade was made before the heat-transfer investigation was begun. The calibration procedure and the method used to correlate the data is presented in reference 7. The final calibration curves, which are presented in reference 7, consisted of plots of $(\rho v)_{a,x}/\mu_{a,w,x}$ against $(p_a^2 - p_{g,x}^2)/\mu_{a,w,x}^2 T_{w,x} \tau_{w,x}$ (Symbols are defined in the appendix.) Plots such as this were made for locations around the blade-wall perimeter that corresponded to the blade-wall thermocouple locations. Before the local cooling-air flows could be determined from the flow-calibration curves it was necessary to determine the local pressure drops across the blade wall for the test conditions of the heat-transfer investigation. The cooling-air pressure on the inside of the blade was measured with the pressure probe that was located inside the blade at a point opposite the blade-wall thermocouple locations. The static pressures on the outside of the porous blade were assumed to be the same as the measured static pressures around an impermeable-wall blade for the same external flow Mach number conditions.

It is shown mathematically in reference 8 that there is practically no difference in temperature between the cooling air and the blade wall at any point within the wall except in a thin section adjacent to the cooling passage due to the large area of metal which is in contact with the cooling air in a porous material. For this reason the measured midwall temperature was taken as the midwall air temperature and used in determining the local cooling-air flows from the calibration curves. The air viscosity, which is involved in the correlation plot, was also evaluated at this temperature.

Correlation of Measured Porous-Blade Temperatures

The effectiveness of any cooling method can be judged by considering the temperature difference ratio $(T_b - T_a)/(T_{g,e} - T_a)$; the greater the effectiveness of the cooling method the lower the value of this ratio will be. Temperatures of impermeable-wall turbine blades operating in a jet engine have been correlated by plotting 1 minus this temperature ratio against the ratio of the cooling-air weight flow rate to the hot-gas weight-flow rate (reference 9). Temperatures of a porous cylinder that was cooled by forcing nitrogen through its walls while hot gases were passing through the inside have also been correlated using the temperature-difference ratio $(T_b - T_a)/(T_{g,e} - T_a)$ (reference 10).

An equation is derived for turbulent flow in references 5 and 6 defining this temperature-difference ratio in terms of the gas Reynolds number, the cooling-air mass velocity, and a gas-to-blade surface heat-transfer coefficient. In the derivation of the equation the flow is considered to be divided into two parts: (1) a very thin laminar sublayer near the wall where the mode of heat-transfer is by conduction; and (2) a turbulent part where the heat-transfer is controlled by turbulent mixing. The resulting ratio presented in reference 6 is in the symbol notation used herein

$$\frac{T_{b,x} - T_a}{T_{g,e} - T_a} = \frac{r}{e^{r\alpha} - 1 + r} \tag{1}$$

where r is the ratio of the velocity parallel to the surface at the hypothetical border between the laminar sublayer and the turbulent part of the boundary layer to the velocity of the stream outside the boundary layer. The value of r that was used in this report was determined according to the relation from Eckert (reference 11)

$$r = \frac{2.11}{(Re_{g,x})^{0.1}} \tag{2}$$

Good correlation of forced-convection heat-transfer coefficients have been obtained by evaluating the property values that occur in the Reynolds number at the wall temperature (reference 12). For this reason the Reynolds number in equation (2) was evaluated as

$$Re_{g,x} = \frac{\rho_{g,b,x}\, v_{g,x}\, x}{\mu_{g,b,x}} \tag{3}$$

The value of α used in equation (1) is defined as

$$\alpha = \frac{(\rho v)_{a,x}\, c_{p,a}}{H'_{c,x}} \tag{4}$$

For turbulent flow with no pressure gradient (flat plate) and for a Prandtl number of 1.0, Colburn (reference 13) presents the following equation for forced-convection heat transfer

$$Nu = 0.0296\ (Re_{g,b,x})^{0.8}\ (Pr_{g,b,x})^{0.333} \tag{5}$$

When this expression for the forced-convection heat-transfer coefficient is substituted in equation (4), the value of α can be expressed as a function of Reynolds number, Prandtl number, and the ratio of local cooling air to combustion-gas mass velocity. The procedure for obtaining this expression follows.

If both sides of equation (5) are divided by Re Pr, it takes the form

$$\frac{Nu}{Re\ Pr} = \frac{H'_{c,x}}{\rho_{g,b,x}\ v_{g,x}\ c_{p,g}} \tag{6}$$

$$\frac{Nu}{Re\ Pr} = \frac{0.0296}{(Re_{g,b,x})^{0.2}\ (Pr_{g,b,x})^{0.667}} \tag{7}$$

If the right side of equation (7) were multiplied by $\rho_{g,b,x}\ v_{g,x}/(\rho v)_{a,x}$ it would be equal to $1/\alpha$.

It is therefore possible to write

$$\alpha = \frac{(Re_{g,b,x})^{0.2}\ (Pr_{g,b,x})^{0.667}}{0.0296}\ \frac{(\rho v)_{a,x}}{\rho_{g,b,x}\ v_{g,x}} \tag{8}$$

A consideration of equation (1) reveals that the temperature-difference ratio is a function of r and α. Since r is a function of Re alone and α is a function of Re and $(\rho v)_{a,x}/\rho_{g,b,x}\ v_{g,x}$, it should be possible to correlate blade-wall temperature data obtained at a constant gas Reynolds number by plotting the temperature-difference ratio $(T_{b,x} - T_a)/(T_{g,e} - T_a)$ against $(\rho v)_{a,x}/\rho_{g,b,x}\ v_{g,x}$. The correlation of the blade-wall temperature data was undertaken following this procedure.

The local blade-wall-surface temperatures were required in the calculation of the temperature-difference ratio. The wall temperatures that were measured were the local temperatures at the midwall. Equations for the wall- and coolant-temperature variation through a transpiration-cooled wall are given in reference 8. The solution of the equations of reference 8 was simplified for use in this report by assuming that the blade-metal and coolant temperatures at any point in the wall were equal. The simplified equation relating the porous-blade surface and midwall temperature is 2383

$$T_{w,x} = T_a + (T_{b,x} - T_a)e^{\frac{-(\rho v)_{a,x}\, c_{p,a} \frac{\tau_{w,x}}{2}}{k_{a,w,x}}} \tag{9}$$

During the investigation reported herein, the maximum difference between the measured midwall temperature and the wall-surface temperature calculated using equation (9) was 63° F.

The effective gas temperature must also be known before the temperature-difference ratio can be determined. The effective gas temperature was determined from the relation

$$\Lambda = \frac{T_{g,e} - T_g}{T'_g - T_g} \tag{10}$$

where Λ is the recovery factor which was assumed equal to 0.90. The gas-total temperature T'_g was that measured in the plenum chamber and the gas static temperature T_g was calculated from the relation

$$\frac{T_g}{T'_g} = \left(\frac{p_g}{p'_g}\right)^{\frac{\gamma_g - 1}{\gamma_g}} \tag{11}$$

The pressure p'_g was the total pressure measured in the plenum chamber and p_g was the static pressure at the cascade inlet.

Calculation of Porous-Blade-Wall Temperatures

Blade-wall temperatures calculated using the equation presented in the preceding section were compared with measured porous-blade-wall temperatures. The following expression was used instead of equation (4) to calculate α:

$$\alpha = \frac{(\rho v)_{a,x}\, c_{p,a}}{H'_{c,x} + H'_{r,x}} \tag{12}$$

where $H'_{r,x}$ is an added coefficient to account for the heat transfer to the blade wall by radiation. The value of $H'_{r,x}$ was determined from the equation

$$H'_{r,x} = \frac{0.173}{(T_{g,e} - T_{b,x})}\left[\left(\frac{T_{g,e}}{100}\right)^4 - \left(\frac{T_{b,x}}{100}\right)^4\right] \tag{13}$$

Since the test section was insulated and only the porous blade was supplied with cooling air, the assumption was made that all surrounding surfaces were at the effective gas temperature $T_{g,e}$. Emissivity and geometry factors of 1.0 were assumed.

In using equations (1) and (12) for calculating porous-blade-wall surface temperature, a trail-and-error method had to be set up since the gas properties needed in the solution of these equations were evaluated at the unknown blade-surface temperature.

The blade-midwall temperatures were then determined from the calculated surface temperatures and equation (9). These calculated midwall temperatures were then compared with the measured midwall temperatures.

Experimental Gas-to-Blade Heat-Transfer Coefficients

Experimental gas-to-blade heat-transfer coefficients for the porous wall were calculated from the data obtained. As pointed out previously, the cooling-air temperature deviated very little from the temperature of a transpiration-cooled wall at any particular location in the wall in the analysis of reference 8. As a consequence, the heat per unit area picked up by the air in passing through the porous blade wall at any local point was set equal to $(\rho v)_{a,x} c_{p,a} (T_{b,x} - T_a)$; $T_{b,x}$ was calculated from the measured midwall temperatures $T_{w,x}$ as explained previously; T_a was the measured air temperature in the blade-coolant passage; and $c_{p,a}$ was evaluated at the measured midwall temperature. This heat was assumed equal to that given up by the hot gas so that the experimental heat-transfer coefficient from gas-to-blade was calculated using the equation

$$H_{c,x} + H_{r,x} = \frac{(\rho v)_{a,x} c_{p,a} (T_{b,x} - T_a)}{(T_{g,e} - T_{b,x})} \tag{14}$$

RESULTS AND DISCUSSION

Determination of Local Cooling-Air Flow Distribution

Calculated cooling-air flow distributions around the porous turbine blade for two ratios of mean coolant weight flow to hot-gas weight flow are shown in figure 6. These flow distributions were obtained following the procedure that is outlined in reference 7. It is significant that there was more cooling air passing through the suction surface than through the pressure surface and that the ratio of the flow through the suction surface to the flow through the pressure surface increased with a decrease in the cooling-air pressure inside the blade. This effect is discussed in reference 7. It is also significant that there was no measurable cooling-air flow through either the leading or the trailing edge of the blade.

Typical Blade Peripheral-Temperature Distributions

Two typical measured peripheral-temperature distributions, which correspond to the two cooling-air flow distributions shown in figure 6, are presented in figure 7. The effect of the low cooling-air flow through the pressure surface at low coolant supply pressures on the blade-wall temperatures is evident when the difference between the suction-surface and pressure-surface temperatures are compared for a value of $(\rho v)_{a,m}/(\rho v)_{g,m}$ of 0.0144. For this cooling-air to combustion-gas flow ratio, the temperature of the suction surface was approximately 400° F and that of the pressure surface about 650° F at the midchord position. The temperatures for the high value of $(\rho v)_{a,m}/(\rho v)_{g,m}$ show that the effect of the pressure variation around the outside of the blade on the cooling-air flow has become less serious along the sides of the blade because these temperatures are more nearly the same on opposite sides of the blade as shown in figure 7. This figure also shows the effect of the lack of cooling air at the leading and trailing edges, which was evident in figure 6. Both the leading- and trailing-edge temperatures are reduced at a value of $(\rho v)_{a,m}/(\rho v)_{g,m}$ of 0.0548 as compared with the temperatures at the low cooling-air flow, but figure 6 shows no air flow through these parts with either flow ratio. The cooling of these parts at the high cooling-air to combustion-gas flow ratio may be a result of conduction from these hot regions to the cooler midchord region of the blade. Furthermore, the trailing edge probably receives some cooling from the air that passes through the wall at the midchord section and flows downstream over the trailing edge.

Comparison of Temperature Distributions of Permeable- and Impermeable-Wall Blades

In order to properly appreciate the effectiveness of a turbine blade that is cooled by the transpiration process, the temperature distribution of the porous blade was compared with that of an impermeable-wall blade, which was cooled by forced convection. The impermeable blade had the same profile as the porous blade and the internal cooling-air surface was increased by brazing ten tubes into the hollow blade shell. The temperature distributions around both blades are compared in figure 8 at a coolant-to-gas flow ratio of 0.04. The data for both blades are experimental data which were obtained in the same cascade for the same operating conditions.

For a gas temperature of approximately 1000° F and a cooling-air temperature of approximately 100° F, the temperature of the ten-tube blade at the midchord region was approximately 530° F and near the leading and trailing edges about 930° and 860° F, respectively. For the porous blade, comparable temperatures on the pressure surface were about 390°, 950°, and 840° F, and on the suction surface, temperatures were 235°, 950°, and 840° F, respectively. The lowest temperature on the porous blade was approximately 170° F, only 70° F higher than the cooling-air temperature. These values point out the possibilities of transpiration cooling as well as the problems which must be overcome. From figure 8, it is apparent that the leading-edge temperatures for about 10 percent of the chord and the trailing-edge temperatures for about 20 percent of the chord are about the same for both blades. The principal means of cooling these portions of both blades seems to be conduction along the blade walls to the cooler midchord regions. Special attention must therefore be directed to the leading-edge and trailing-edge regions of transpiration-cooled turbine blades as well as to the pressure surface in an effort to increase the coolant flow there and approach the excellent cooling conditions attained on the suction surface of the present blade at a low cooling-air flow rate. Further investigations are necessary in order to determine whether local changes in permeability around the blade as well as changes in blade design, which are acceptable aerodynamically, will result in more uniform temperature distributions. Such investigations are well warranted on porous blades on the basis of the very effective cooling results on some parts of the present blade. On the premise that a transpiration-cooled blade had the same cooling effectiveness over all of its surface as that of the suction surface of the present blade at the 30-percent chord position (fig. 8) at a gas temperature of 5000° F and a cooling-air temperature of 500° F, the blade temperature would be about 900° F.

In addition to further investigations on porous blades to improve the over-all cooling characteristics, work must be done to improve the strength characteristics of materials made by powder metallurgy in order to use them for turbine-rotor blades. The strength of present porous materials is insufficient for use in turbine-rotor blades but work is underway at Stevens Institute of Technology for the Bureau of Aeronautics of the Navy (reference 14) and at Rensselaer Polytechnic Institute for the Bureau of Aeronautics (reference 15) to improve the strength of such materials.

Correlation of Porous-Blade Temperature

The correlation of the porous-blade-wall temperatures was attempted by plotting the ratio of coolant weight flow to combustion-gas weight flow against the temperature difference ratio $(T_{b,x} - T_a)/(T_{g,e} - T_a)$. Correlation curves were obtained for the wall-temperature data for four locations on the blade for varying gas temperature and weight flow. Curves for these locations are shown in figure 9. The temperature data that were obtained at various gas temperatures but at a constant gas weight flow correlated along a single curve (fig. 9(a)). The data obtained at various gas weight flows at a constant gas temperature did not correlate along a single curve (fig. 9(b)). This might be expected because the temperature-difference ratio is a function of gas Reynolds number as was pointed out in the ANALYSIS. However, the data scattered considerably and no definite trends with varying gas Reynolds number could be established. The curves for locations 2, 7, and 8 are almost identical. A mean curve drawn for these locations would therefore be sufficiently accurate for design purposes. The curve for location 3 shows that this location was cooled more effectively than any of the other three locations. This may be a result of separation which possibly occurs at this location on the blade. Before definite trends of the temperature-difference ratio $(T_{b,x} - T_a)/(T_{g,e} - T_a)$ with variations in the gas Reynolds number can be established much more data will be required.

Comparison of Calculated and Measured Blade Temperatures

A comparison of the porous-blade midwall temperatures calculated by methods given previously with measured values are shown for two locations on the blade; one a location near the trailing edge on the pressure surface (thermocouple 7, fig. 10(a)), and the other a comparable position on the suction surface (thermocouple 3, fig. 10(b)). A 45° line has been drawn on each figure and if the temperature points fall on this line, perfect agreement between calculated and measured values is indicated. Figure 10(a) shows that at low blade-wall temperatures, that is, high cooling-air weight flows, the predicted and measured temperatures agreed well; but as the wall temperature increased, the calculated temperature became greater than the measured temperature. At a measured wall temperature of about 580° F the calculated temperature was approximately 740° F. The relation between calculated and measured wall temperatures for thermocouple locations 2 and 8 were the same as that shown in figure 10(a). The comparison between calculated and measured wall temperatures for thermocouple location 3 is shown in figure 10(b). For this one location on the blade, the agreement between calculated and measured wall temperatures was good over the entire temperature range. The variation of this result from those of the other thermocouple locations may be caused by a possible flow separation at this point on the blade surface.

There are several factors which may affect the accuracy of the temperature predictions that were made. Solutions for turbulent boundary-layer heat transfer are not exact, consequently some of the assumptions under which equation (1) was derived in reference 6 may not have been completely valid in this case. Equation (1) was derived for the case of the gas and the coolant having a Prandtl number of 1.0 and for a plane wall with a zero pressure gradient in the direction of gas flow. These assumptions may introduce some error in the blade-wall temperature predictions where the gas and the coolant Prandtl numbers were less than 1.0 and there was a pressure gradient in the direction of gas flow. Other possible factors that may affect the accuracy of the temperature predictions arise from the calculation procedure that was followed. One factor is the accuracy with which the local cooling-air flow rates could be determined. These may have been slightly inaccurate because the local static pressure around the outside of the blade was obtained from an impermeable-wall blade. This outside static pressure was used with the measured inside pressure in order to determine the pressure drop across the wall for use in the determination of the local cooling-air flows.

Another possible source of error in the calculated temperatures is the correction that was made for radiation. The porous blade received radiant heat from the uncooled blades on either side of it and from the surrounding insulated test section. A rough correction was made for this effect by the assumption that the surrounding surfaces were at the effective gas temperature and that the emissivity and geometry factors were 1. With the complicated shapes involved, some error probably resulted through the use of such assumptions. The maximum correction for radiation occurred at a gas temperature of 1000° F with high cooling-air flow rates. For this condition the correction to the outside heat-transfer coefficient was about 15 percent. The minimum correction occurred at a gas temperature of 300° F for the low cooling-air flow rates. For this condition, the correction to the outside convection heat-transfer coefficient was approximately 2 percent.

2383

Experimental Gas-to-Blade Heat-Transfer Coefficients

Experimental heat-transfer coefficients for the transpiration-cooled blade wall and the calculated forced-convection heat-transfer coefficients for an impermeable wall having the same temperature as the porous wall are compared in figure 11. The heat-transfer coefficients were determined for a gas weight flow over a range of cooling-air weight flows $(\rho v)_{a,x}$ for four thermocouple locations.

Equation (14) was used for determining the experimental $H'_{c,x} + H'_{r,x}$. Each set of results for each thermocouple location is shown on a separate portion of the figure. Also shown in the figure are the calculated values of $H_{c,x} + H_{r,x}$ for each location, which were obtained using equations (5) and (13). These values represent heat-transfer coefficients for an impermeable surface with the same surface temperature as the permeable one.

The heat-transfer coefficient that is obtained when the experimental local heat-transfer coefficients for a porous blade are extrapolated to the point of zero cooling-air flow is the coefficient that would exist for a solid wall under the gas-flow conditions of these tests. This procedure was followed in reference 6 for a porous cylinder and the results agreed well with established heat-transfer relations for flow through an impermeable-wall cylinder. The heat-transfer coefficients that were used in the calculations of the blade-wall temperatures are shown in figure 11 by the dashed line. The value of the heat-transfer coefficient increases as the cooling-air flow increases because the gas properties that were used in equation (5) were based on the local blade-wall temperature. Both the experimental and the calculated curve should extrapolate to the same value at zero cooling-air weight flow. The curves for locations 2 and 3 do extrapolate to approximately the same coefficient at zero cooling-air flow but locations 7 and 8 drop off very rapidly and do not even approach the value of the zero heat-transfer coefficient as calculated using equations (5) and (13). This dropping off is probably the result of locations 7 and 8 being on the pressure surface of the blade where there are very low cooling-air pressure drops and the accurate determination of the pressure drop and the cooling-air weight flow is difficult. Also, an unstable boundary layer might prevail along the pressure surface.

The heat-transfer coefficient which was suggested for use in reference 6 is the coefficient at zero cooling-air weight flow, but this constant coefficient does not take into account any variations in the ratio of the gas temperature to the blade temperature. The effect of this gas-to-blade temperature ratio has been shown to be quite pronounced in reference 3 for the case of laminar flow over a porous material. The use of equation (5) for determining the heat-transfer coefficients partly accounts for this temperature ratio. It was for this reason that this value of the heat-transfer coefficient was used in the calculation of the blade-wall temperatures.

The curves of the calculated and the experimental heat-transfer coefficients point out the need for more information on the heat-transfer coefficients for a porous material. Experimental work is needed to investigate the effect of the gas-to-blade temperature ratio both in the laminar-flow region and in the turbulent-flow region and refinements may be required in the turbulent-flow heat-transfer theory for transpiration cooling. Another effect which should be studied is the effect of surface roughness on the heat-transfer coefficient for a porous material. These two factors must be evaluated before any accurate calculations of turbine-blade-wall temperatures can be made.

SUMMARY OF RESULTS

An investigation was conducted in a static cascade at gas temperatures of 300°, 600°, and 1000° F to determine the heat-transfer characteristics of an air-cooled porous turbine blade. The results of the investigation are summarized as follows:

1. Temperature distributions around the blade showed excellent cooling at the midchord locations on the blade but poor cooling at the leading and trailing edges resulting from a poor cooling-air distribution on this blade.

2. Transpiration cooling promises to be a more effective method of cooling turbine blades than convection cooling. Comparison of the minimum temperatures on a porous blade and a ten-tube convection cooled blade for a gas temperature of approximately 1000° F, a cooling-air temperature of approximately 100° F, and a ratio of cooling-air mass velocity to combustion gas flow of 0.04 showed that the coolest location on the porous blade was 170° F, whereas the coolest location on the convection cooled blade was 530° F.

3. The method of blade-temperature correlation on the basis of plotting a nondimensional temperature-difference ratio against cooling- 2383
air to combustion-gas mass-velocity ratio gave a correlation of the blade-wall temperature data obtained at different combustion-gas temperatures. The data obtained at different combustion-gas Reynolds numbers scattered slightly but the correlation method should still be useful for design purposes.

4. The blade-wall temperatures measured were generally lower than the wall temperatures calculated by using the turbulent-flow equations presently available. The difference between the values decreased with increasing cooling-air flow rates.

Lewis Flight Propulsion Laboratory
National Advisory Committee for Aeronautics
Cleveland, Ohio

APPENDIX

SYMBOLS

The following symbols are used in this report:

c_p specific heat at constant pressure, Btu/(lb)(°F)

H heat-transfer coefficient for porous blade on hot-gas side, Btu/(hr)(sq ft)(°F)

H' heat-transfer coefficient for impermeable-wall blade, Btu/(hr)(sq ft)(°F)

k thermal conductivity, Btu/(°F)(ft)(sec)

Nu Nusselt number, $H'x/k$

p static pressure, lb/sq ft

p' total pressure, lb/sq ft

Pr Prandtl number, $c_p \mu g/k$

Re Reynolds number, $\rho vx/\mu$

r ratio of velocities in boundary layer, (equation (1))

T static temperature, °R

T' total temperature, °R

v velocity, ft/sec

W weight flow rate, lb/sec

x peripheral distance along blade surface from leading edge to particular thermocouple location, ft

α parameter used in equation (1)

γ ratio of specific heats, c_p/c_v

Λ temperature-recovery factor

μ viscosity, lb-sec/sq ft

ρ density, lb/cu ft

τ thickness, ft

Subscripts:

a air inside blade at midspan location

b blade surface, hot gas side

c convection

e effective

g combustion gas

m mean

r radiation

w midwall (when used with temperature, denotes blade temperature at midwall position)

x local (refers to condition at distance x from leading edge in direction of gas flow)

REFERENCES

1. Canright, Richard B.: Preliminary Experiments of Gaseous Transpiration Cooling of Rocket Motors. Prog. Rep. No. 1-75, Power Plant Lab. Proj. No. MX801, Jet Prop. Lab., C.I.T., Nov. 24, 1948. (AMC Contract No. W-535-ac-20260, Ordnance Dept. Contract No. W-04-200-ORD-455.)

2. Eckert, E. R. G., and Esgar, Jack B.: Survey of Advantages and Problems Associated with Transpiration Cooling and Film Cooling of Gas-Turbine Blades. NACA RM E50K15, 1951.

3. Brown, W. Byron: Exact Solutions of the Laminar Boundary Layer Equations for a Porous Plate with Variable Fluid Properties and a Pressure Gradient in the Main Stream. Paper presented at First U. S. National Congress of Applied Mechanics (Chicago), June 11-16, 1951.

4. Eckert, E. R. G., and Livingood, John N. B.: Calculation of Laminar Heat Transfer Around Cylinders of Arbitrary Cross Section and Transpiration-Cooled Walls with Application to Turbine Blade Cooling. NACA RM E51F22, 1951.

5. Rannie, W. D.: A Simplified Theory of Porous Wall Cooling. Prog. Rep. No. 4-50, Power Plant Lab. Proj. No. MX801, Jet Prop. Lab., C.I.T., Nov. 24, 1947. (AMC Contract No. W-535-ac-20260, Ordnance Dept. Contract No. W-04-200-ORD-455.)

6. Friedman, Joseph: A Theoretical and Experimental Investigation of Rocket-Motor Sweat Cooling. Jour. Am. Rocket Soc., no. 79, Dec. 1949, pp. 147-154.

7. Bartoo, Edward R., Schafer, Louis J., Jr., and Richards, Hadley T.: Experimental Investigation of Coolant-Flow Characteristics of a Sintered Porous Turbine Blade. NACA RM E51K02 , 1952.

8. Weinbaum, S., and Wheeler, H. L., Jr.: Heat Transfer in Sweat-Cooled Porous Metals. Prog. Rep. No. 1-58, Air Lab. Proj. No. MX121, Jet Prop. Lab., C.I.T., April 8, 1947. (AMC Contract No. W-535-ac-20260, Ordnance Dept. Contract No. W-04-200-ORD-455.)

9. Arne, Vernon L., and Esgar, Jack B.: Experimental Investigation of Air-Cooled Turbine Blades in Turbojet Engine. VI - Conduction and Film Cooling of Leading and Trailing Edges of Rotor Blades. NACA RM E51C29, 1951.

10. Duwez, Pol, and Wheeler, H. L., Jr.: Heat-Transfer Measurements in a Nitrogen Sweat-Cooled Porous Tube. Prog. Rep. No. 4-48, Power Plant Lab. Proj. No. MX801, Jet Prop. Lab., C.I.T., Nov. 6, 1947. (AMC Contract No. W-535-ac-20260, Ordnance Dept. Contract No. W-04-200-ORD-455.)

11. Eckert, E. R. G.: Introduction to the Transfer of Heat and Mass. McGraw-Hill Book Co., Inc., 1950.

12. Lowdermilk, Warren H., and Grele, Milton D.: Heat Transfer from High-Temperature Surfaces to Fluids. II - Correlation of Heat-Transfer and Friction Data for Air Flowing in Inconel Tube with Rounded Entrance. NACA RM E8L03, 1949.

13. Colburn, Allan P.: A Method of Correlating Forced Convection Heat Transfer Data and a Comparison with Fluid Friction. Trans. Am. Inst. Chem. Eng., vol. XXIX, 1933, pp. 174-210.

14. Comstock, Gregory J., et al.: Navy Project for Investigation of Porous Material from Spherical Metal Powders. Bi-Monthly Progress Report #5, Stevens Institute of Technology, June 1, 1951 to July 31, 1951. (Navy BuAer Contract NOas-51-185-C.)

15. Hill, M., Reen, O. W., Vermilyea, D. A., and Lenel, F. V.: Production of Porous Metal Compacts. Bi-Monthly Prog. Rep. No. 3, Powder Metallurgy Lab., Rensselaer Polytechnic Institute, Oct. 6, 1950. (Navy Res. Contract NOa(s) 11022.)

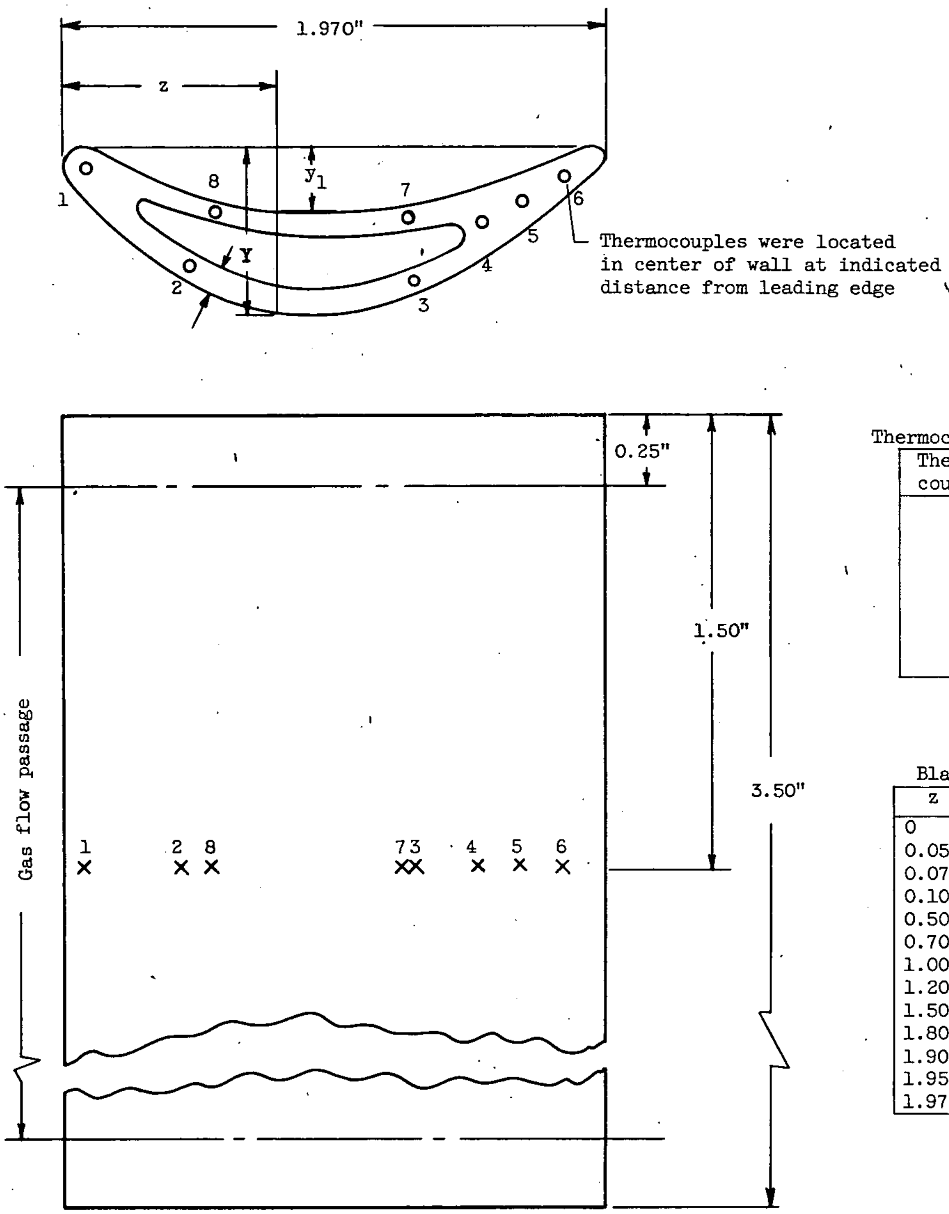

Thermocouple locations

Thermo-couple	z
1	0.06
2	0.43
3	1.29
4	1.51
5	1.67
6	1.83
7	1.26
8	0.53

Blade coordinates

z	y	y_1
0	0.064	0.064
0.050	0.166	0.002
0.075	0.202	0.002
0.100	0.237	0.014
0.500	0.548	0.187
0.700	0.614	0.235
1.000	0.632	0.260
1.200	0.600	0.252
1.500	0.461	0.195
1.800	0.214	0.082
1.900	0.117	0.019
1.950	0.064	0.002
1.970	0.032	0.032

Figure 1. - Blade dimensions and thermocouple locations.

[redacted]

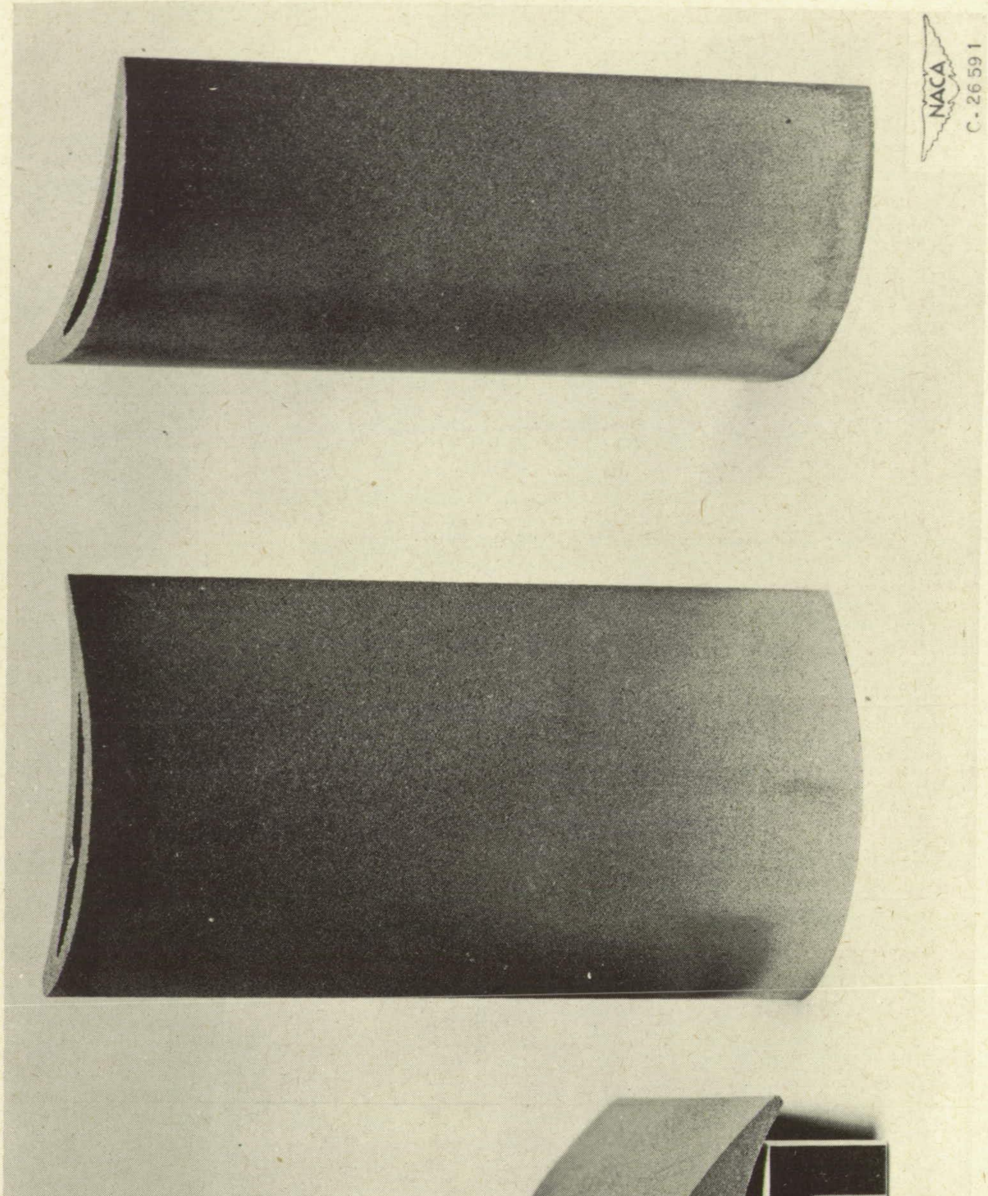

Figure 2. - Porous stainless-steel turbine blades.

[redacted]

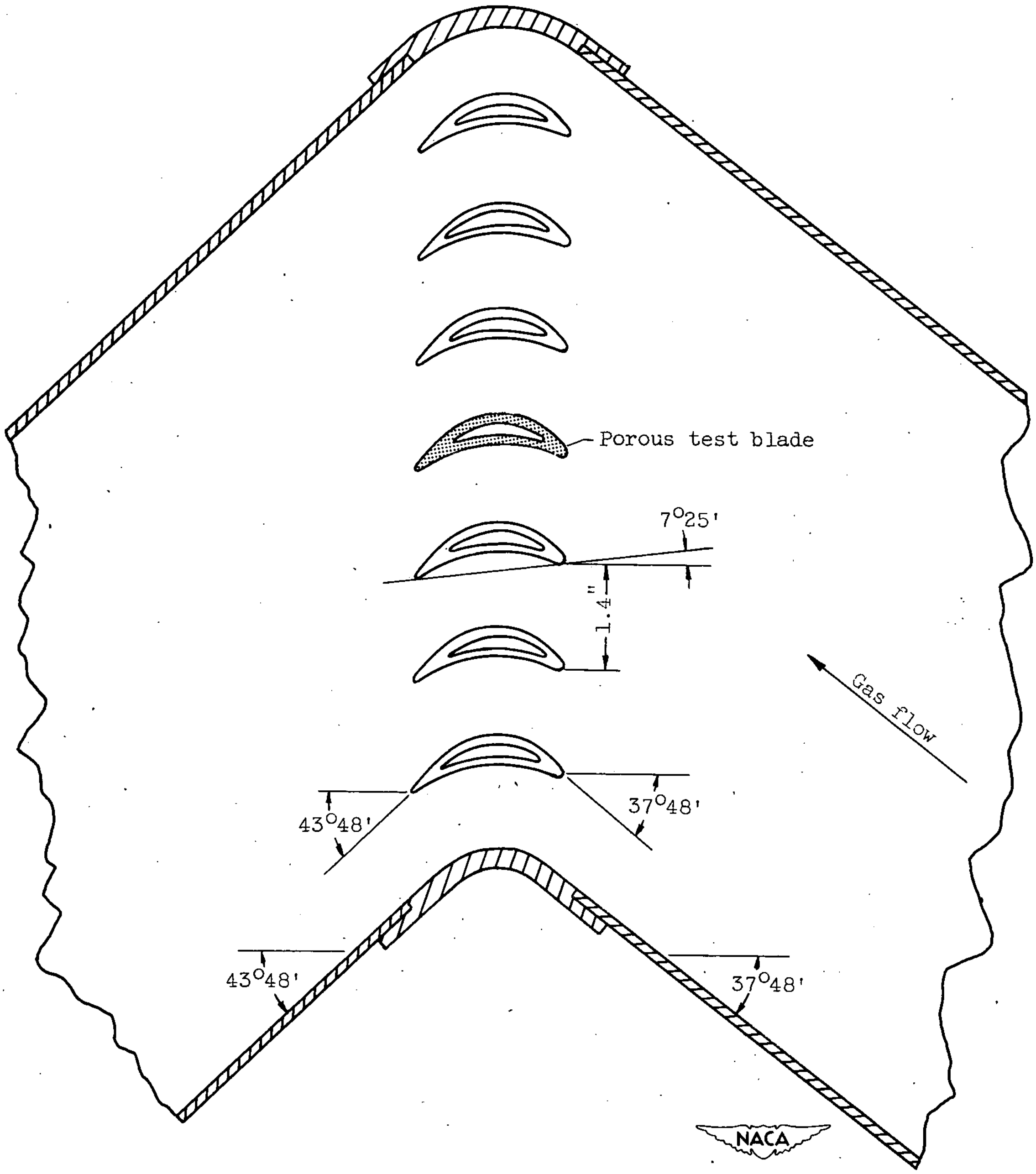

Figure 3. - Cascade geometry.

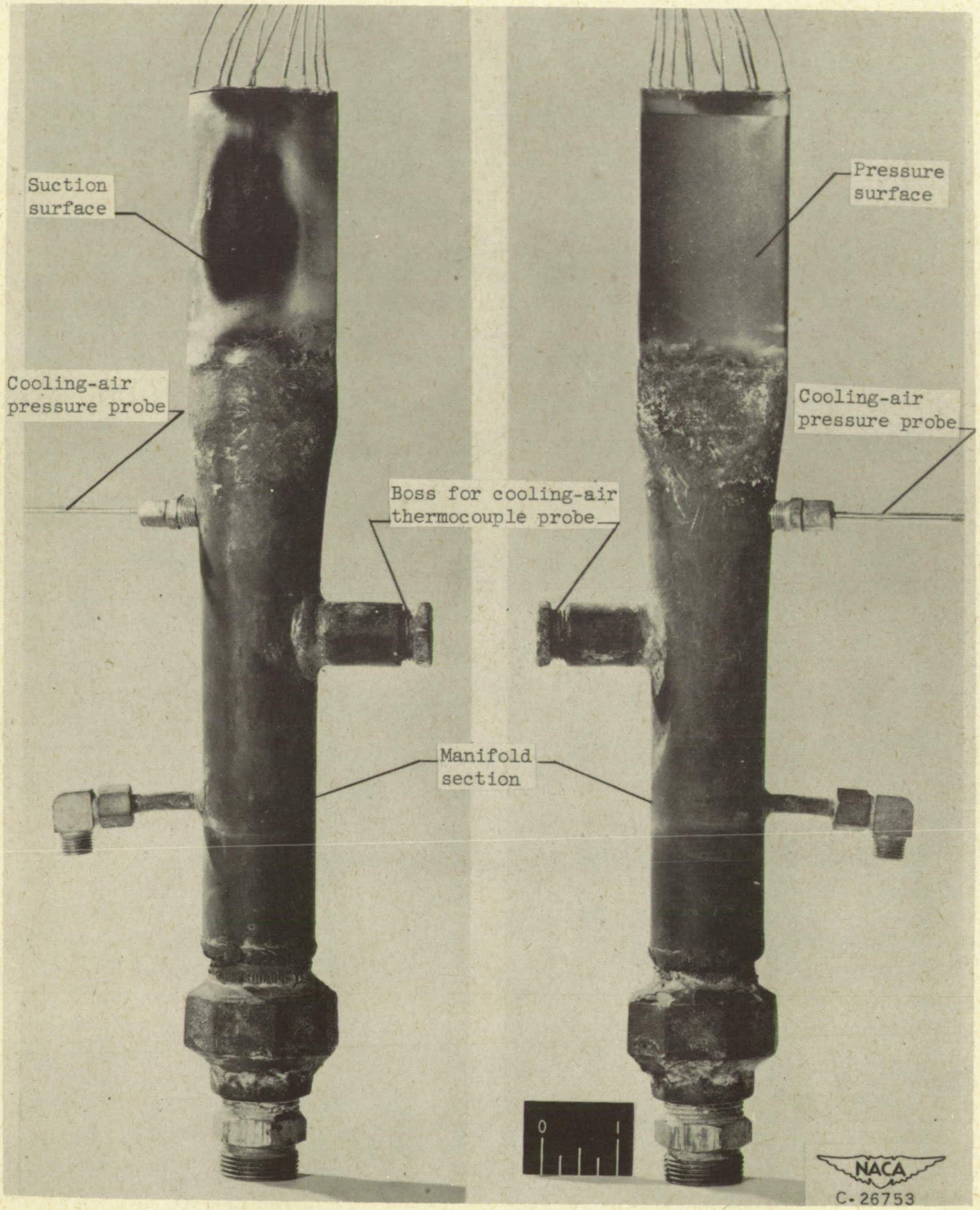

Figure 4. - Porous blade with cooling manifold attached.

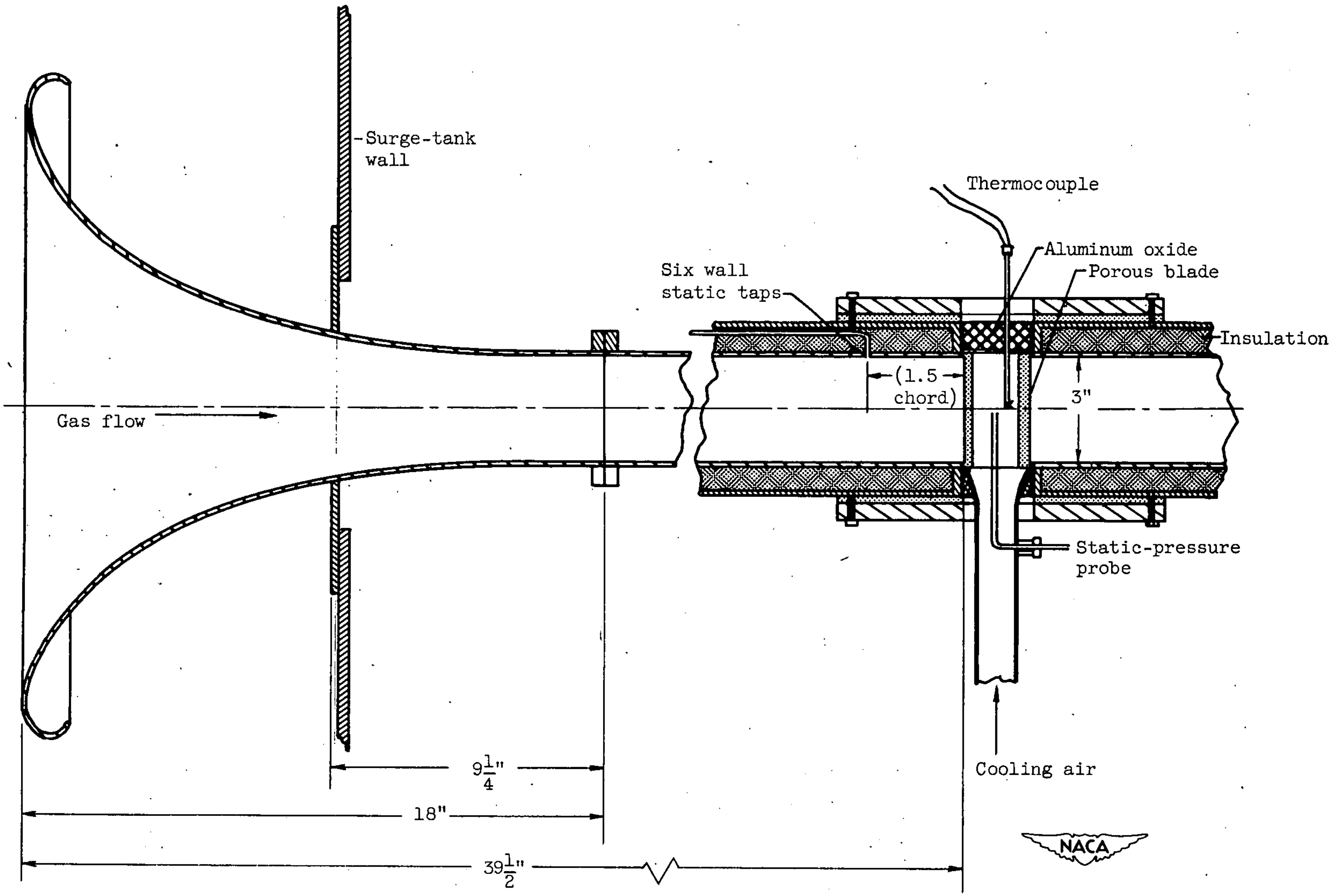

Figure 5. - Sectional view of heat-transfer test section showing instrumentation.

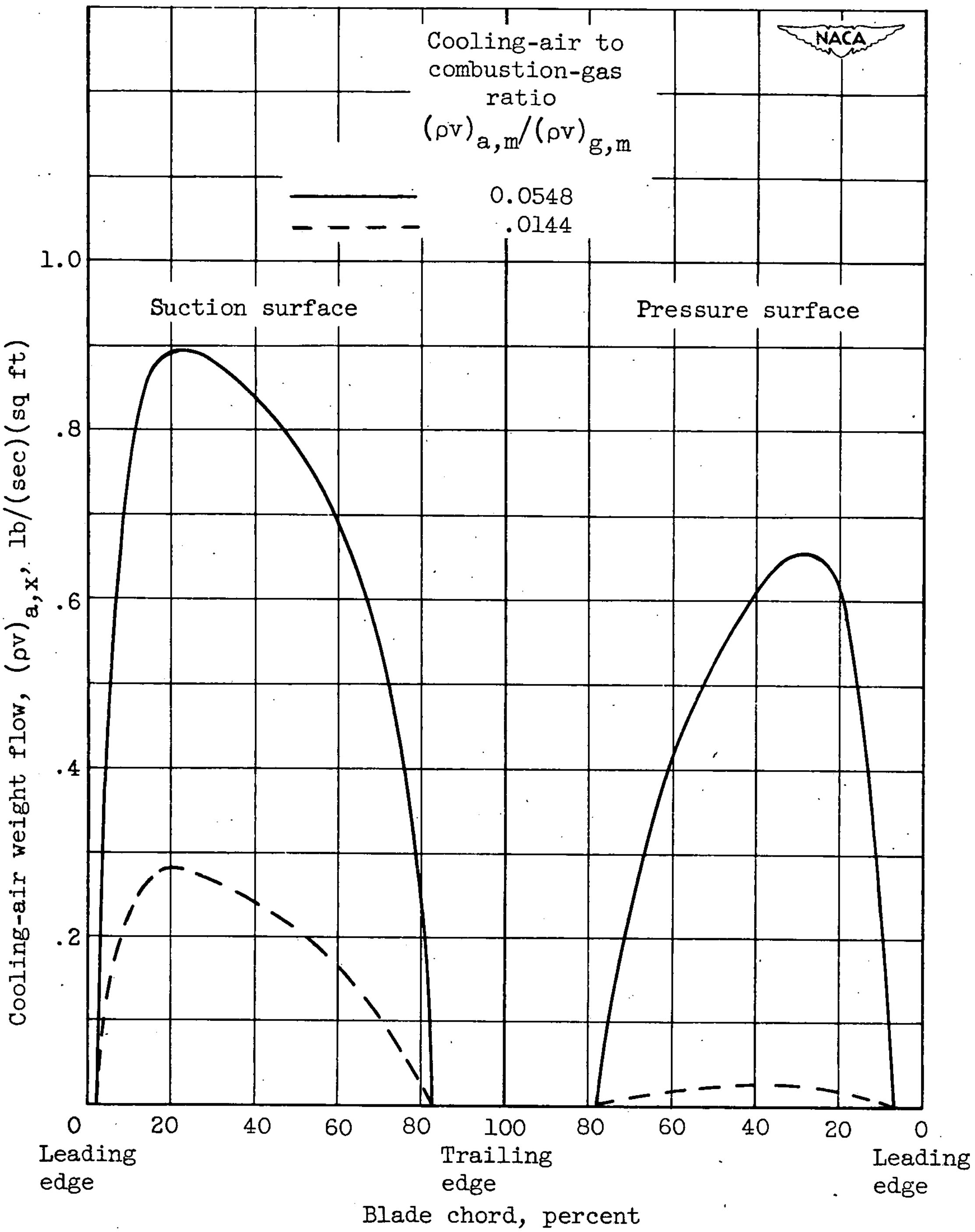

Figure 6. - Two typical coolant-flow distributions around blade perimeter in 1000° F gas stream at Mach number of 0.45. Gas weight flow, 4 pounds per second; mean combustion-gas weight flow, 24.05 pounds per second per square foot.

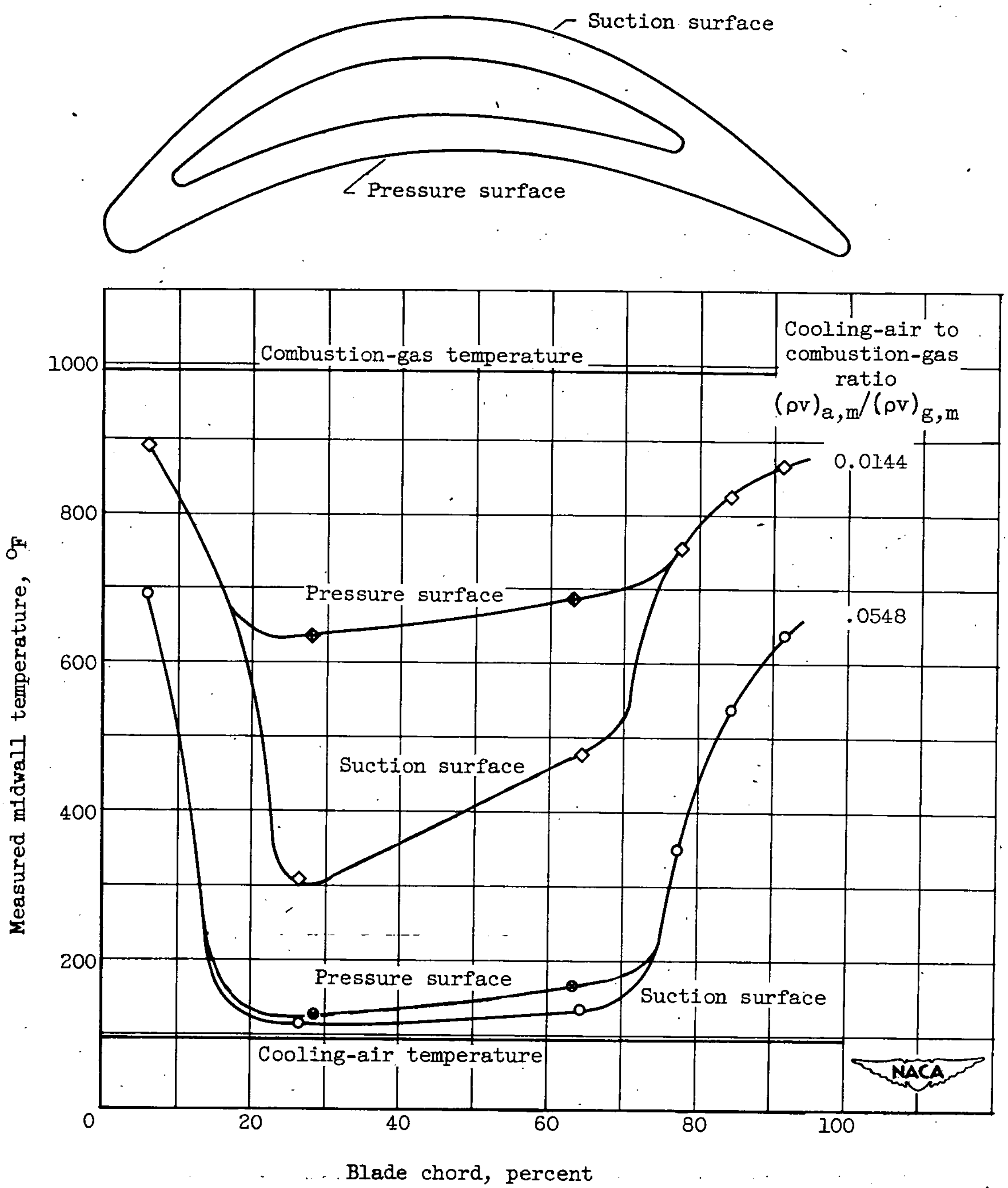

Figure 7. - Peripheral-temperature distributions on a porous turbine blade at two cooling-air flows. Gas weight flow, 4 pounds per second.

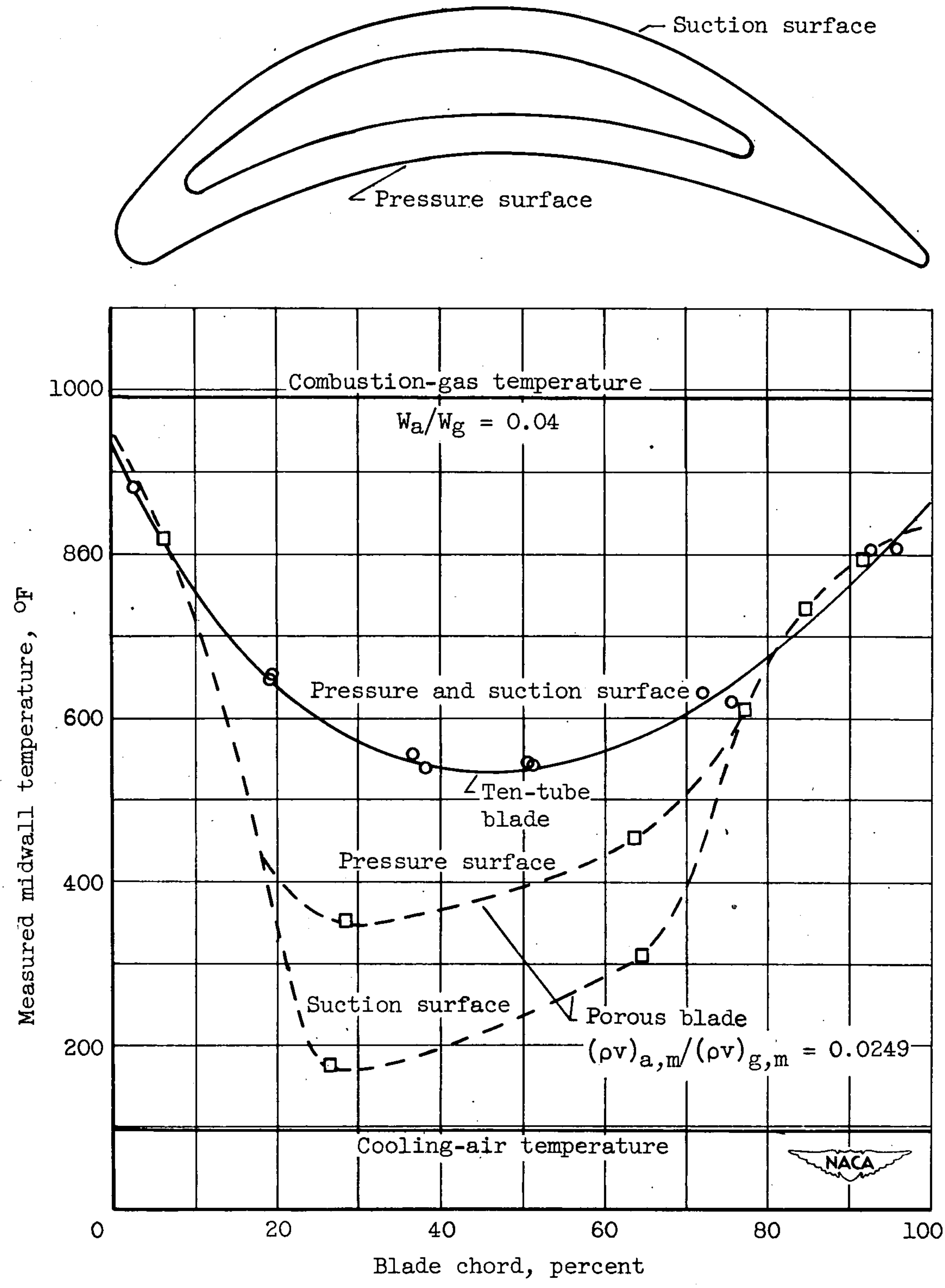

Figure 8. - Comparison of porous-blade peripheral-temperature distribution with temperature distribution of ten-tube blade.

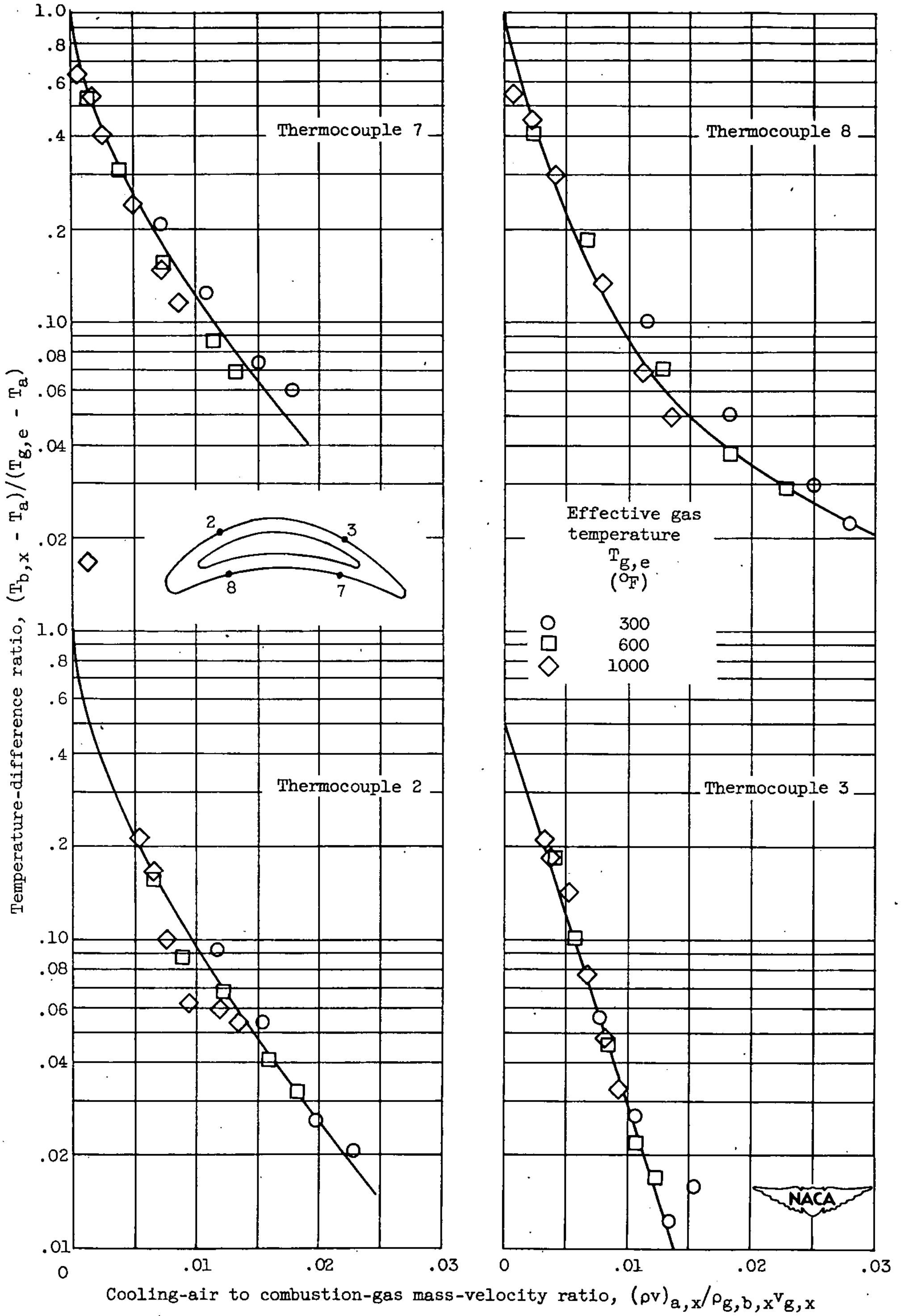

(a) Temperature-difference ratio for several gas temperatures.
Gas weight flow, 4 pounds per second.

Figure 9. - Temperature-difference ratio for various locations, gas weight flows, and gas temperatures.

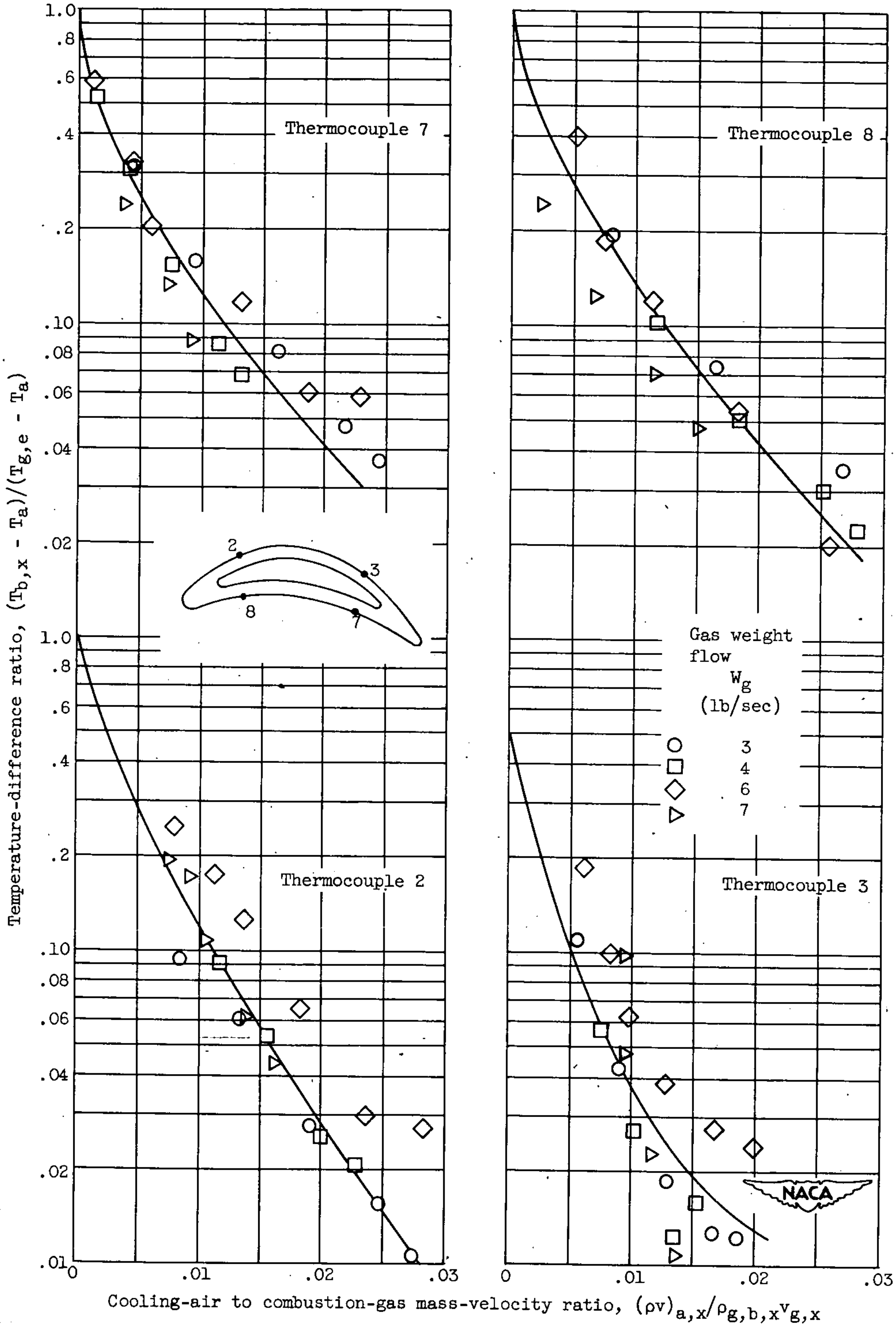

(b) Temperature-difference ratio for several gas weight flows. Effective gas temperature, 300° F.

Figure 9. - Concluded. Temperature-difference ratio for various locations, gas weight flows, and gas temperatures.

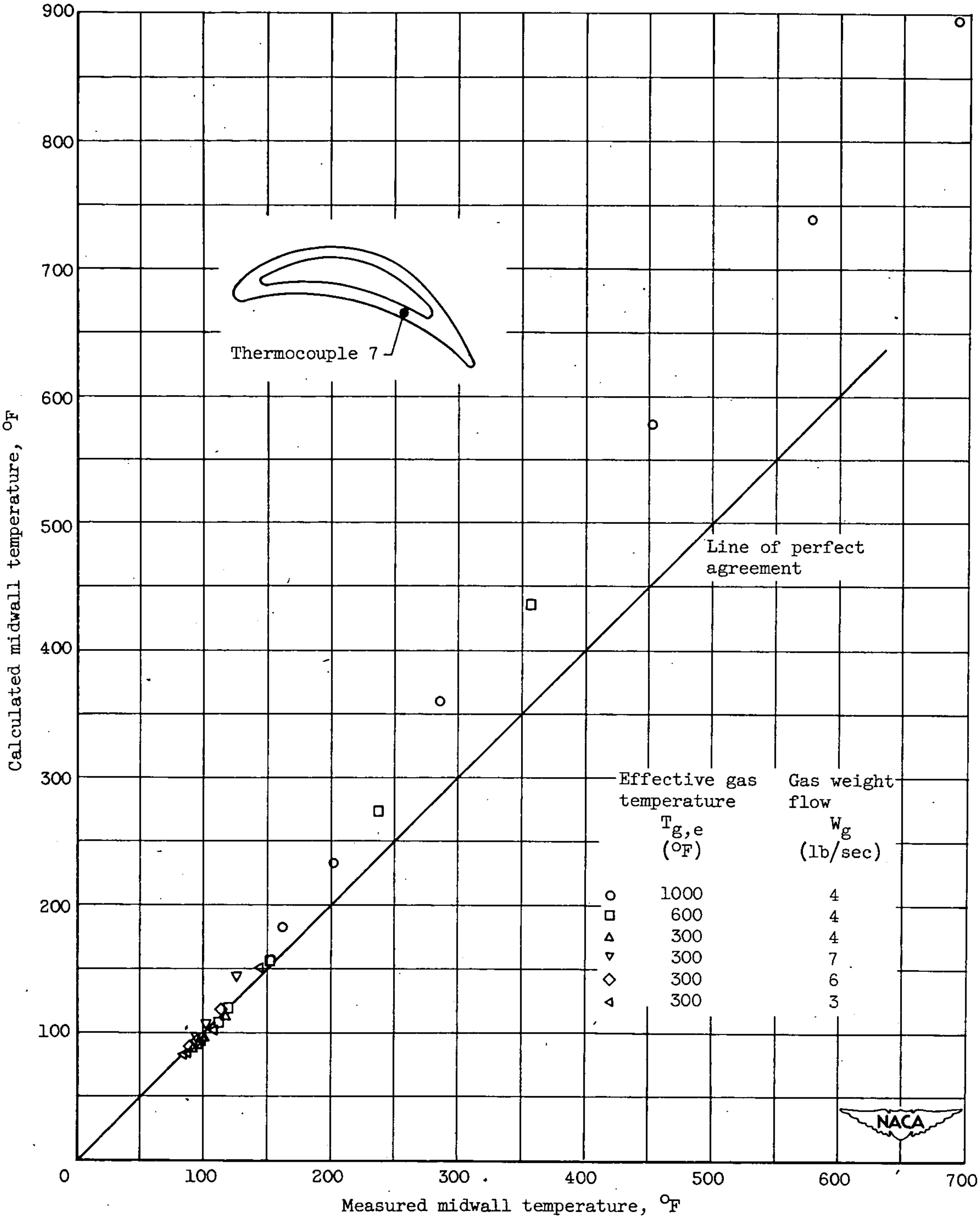

(a) Thermocouple 7.

Figure 10. - Comparison of calculated and measured blade-wall temperatures with varying cooling-air weight flow and combustion-gas temperature.

[redacted]

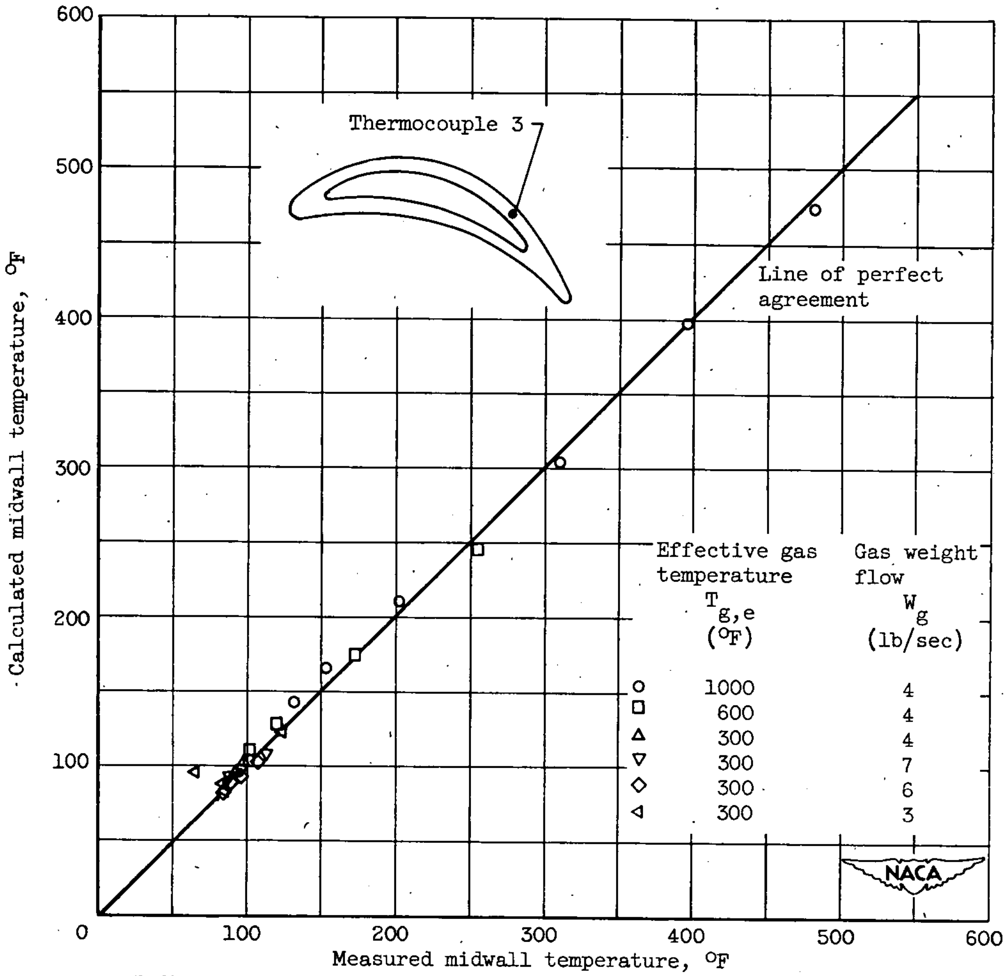

(b) Thermocouple 3.

Figure 10. - Concluded. Comparison of calculated and measured blade-wall temperatures with varying cooling-air weight flow and combustion-gas temperature.

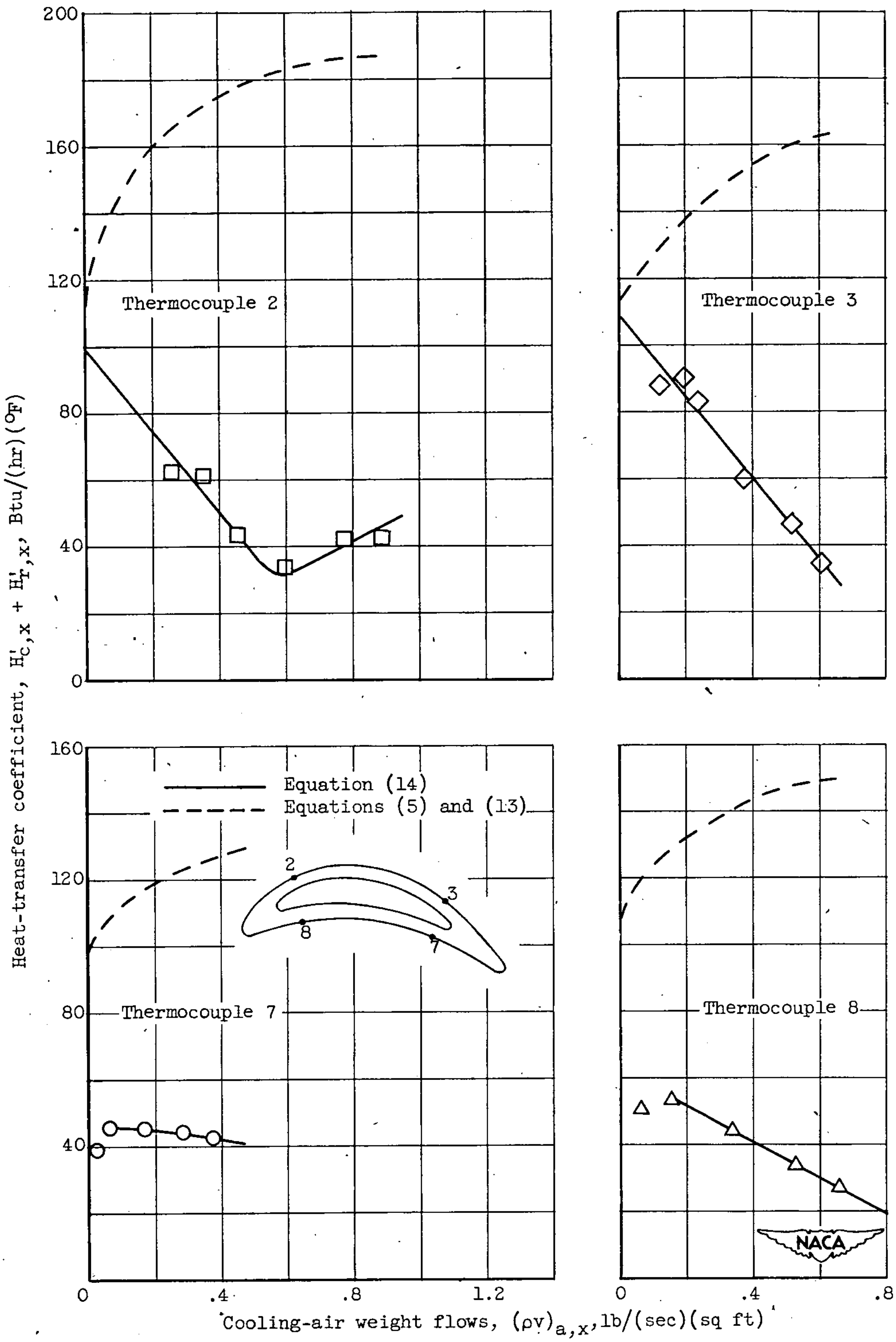

Figure 11. - Local gas-to-blade heat-transfer coefficients at different coolant flows for four blade thermocouple locations. Effective gas temperature, 993° F; gas weight flow, 4 pounds per second.

NACA-Langley - 2-5-52 - 450